

# STRESS INTENSITY FACTOR SOLUTIONS FOR ARBITRARILY SHAPED SURFACE FLAWS IN REACTOR PRESSURE VESSEL NOZZLE CORNERS

S. N. ATLURI, K. KATHIRESAN

*Georgia Institute of Technology, School of Engineering Science and Mechanics,  
225 North Avenue, Atlanta, Georgia 30332, U.S.A.*

## SUMMARY

Extensive experimental results, based on frozen stress photoelasticity technique for extracting stress intensities, for nozzle corner cracks in ITV and BWR geometries were reported by C. W. Smith (Paper No. G4/3, 4th SMIRT). Based on the above experimental studies, it was conjectured that if the crack shape inserted into a finite element model is not a real one, or if the inner fillet (for shallow flaws) or the outer boundary shape (for moderate to deep flaws) is improperly approximated, the obtained numerical results for stress intensity factors may differ significantly from the physical behavior at the nozzle-vessel juncture. On the other hand almost all the numerical analyses published to date, based on finite elements, or boundary integral equations, or alternating techniques, considered only quarter-circular nozzle-corner cracks.

This paper presents stress-intensity factor solutions for natural shaped nozzle-corner cracks in pressurized ITV and BWR vessels. Several actual crack geometries observed in the above cited experimental work of C. W. Smith are studied, using the three-dimensional hybrid crack-element approach of Atluri et al (Paper L-7/3, 3rd SMIRT; and Paper G-5/4, 4th SMIRT), wherein the stress-intensity factors and their variation along an arbitrarily shaped 3-D crack front are directly computed. In order to be able to compare the present results with the photoelastic experimental results (wherein the Poisson's ratio of the material is 0.5), some of the present numerical results are obtained for  $\nu \approx 0.5$ .

Also, in the paper some new solutions for stress-intensity factors for pressurized thin (outer to inner radii ratios of  $\sim 1.1$ ) cylindrical vessels with belt-line flaws of semi-elliptical shapes of various aspect ratios and depth ratios are presented. The cases of surface flaws in the meridional direction as well as circumferential direction of the vessel are treated.

1. Introduction: A complex structural mechanics problem in nuclear pressure vessels is the stress analysis of pressure-vessel-nozzle juncture. Incorporation of these inlet and outlet nozzles being unavoidable for the operation of the pressure vessels for their intended application, they introduce complex and high stress gradients near the nozzle juncture. Also, to further complicate the situation, corner cracks are often found to be present at the intersection of pressure vessel and nozzle. The fracture analysis of such nozzle corner cracks in pressure vessels is very important and critical for efficient design and assessment of structural integrity of the pressure vessels. Recently, considerable amount of attention has been paid to these problems by analytical as well as experimental investigators. Smith et al [1] made an extensive experimental study of nozzle corner cracks in ITV, BWR and flat plate geometries, using the frozen stress photoelasticity technique. A three-dimensional crack analysis of LWR nozzle-cylinder intersection using special singularity elements and virtual crack extension method was carried out by Hellen and Dowling [2]. Broekhoven [3] computed the stress intensity factors for nozzle corner cracks by various finite element procedures and compared the solutions. Broekhoven [4] also conducted some experimental investigation of fatigue and fracture behaviour of nozzle corner cracks and compared them with theoretically predicted solutions. Similar experimental work on fatigue behaviour of LWR pressure vessels was done by Miyazono et al [5]. Finite element methods using special singularity element and/or virtual crack extension method were also used by Schmitt et al [6], and Reynen [7] for the solution of nozzle corner cracks. In almost all of the prior works on nozzle corner cracks using numerical procedures such as finite element method, alternating technique, etc., the crack shapes were assumed either quarter-circular or quarter-elliptical in geometry. However, in all the experimental studies, it was observed that the real crack shape is significantly different from that which is mathematically describable as a quarter-circular or quarter-elliptical shape.

In this paper, the three-dimensional hybrid displacement special crack front element developed by Atluri et al [8,9] is utilized to solve the nozzle corner crack problems in pressurized BWR as well as ITV pressure vessels. Unlike the previous investigations, in the present analysis, 'natural' flaw shapes as observed in experiments [1] are inserted in the finite element solution procedure. Care has also been exercised to model the inner fillet and the outer boundary shape of nozzle accurately.

Turning now to a second category of somewhat easier problems, pressure vessels with semi-elliptical surface flaws in meridional direction were analyzed by McGowan and Raymond [10] using a finite element technique with Parks' stiffness derivative method and by Heliot et al [11] using boundary integral equation method. In these analyses, Refs. [10,11] examined the crack shapes recommended by ASME Boiler and Pressure Vessel Code [12]. A special singular finite element procedure was used by Raju and Newman [13] for the solution of semi-elliptical surface flaws in thin plates. The present hybrid displacement finite element procedure is also used to solve pressure vessel problems identical to those considered in [10,11] and thin plate problems similar to those considered in [13] and the solutions are compared. Solutions for circumferential belt-line surface flaws are also presented in the present paper; comparison results for this class of problems have so far not appeared in literature.

2. Formulation: The presently used hybrid displacement finite element procedure is well documented in open literature and the reader is referred to the earlier works of Atluri et

a1 [8,9,14] for detailed information on the formulation and assumed field variables. It is possible, as explained in [8,9,14], that in this procedure, both the nodal displacements, as well as the three mixed-mode stress-intensity factors at various points along the crack front, can be directly solved for. Thus this procedure is fundamentally in contrast with indirect methods of obtaining  $k_s^*$ , such as by using procedures of extrapolation from computed finite element solutions of stresses or displacements.

**3.1 Surface Flaws in Thin Plates:** A convergence study for the solution of semi-elliptical surface flaws in thin plates, using Tracey's [15] wedge shaped distorted isoparametric crack elements, was done by Raju and Newman [13] for different ratios of crack depth to thickness. For identical problems, similar convergence study was also carried out using the present hybrid finite element procedure. The problem geometry and the solution of normalized stress intensity factors for crack depth to plate thickness ratios of .6 and .8 are presented in Figs. 1 and 2 respectively. In Figs. 1 and 2, the solutions of Raju and Newman [13] corresponding to their highest degrees of freedom (6867) and the solutions by the present method with three different degrees of freedom (4151, 4353 and 4555 after imposing the boundary conditions) are presented. The present solution also agrees excellently with that of Raju and Newman [13]. Thus it can be seen that the present procedure yields accurate results for K factors directly (instead of relying on extrapolation procedures) even with fewer degrees of freedom of the finite element model.

**3.2 Fracture Problems With Known Exact Solution:** The present procedure was also used to solve some simple fracture problems whose exact analytical solutions are available. First a through-the-thickness axial crack in a pressurized thin cylindrical shell ( $R/t = 25$ ) considered by Erdogan [16] was solved. The crack length  $2a$  was assumed such that  $a/\sqrt{Rt} = 2$ . The analytical exact solution for the normalized (by  $\sigma_{\text{memb}}\sqrt{\pi a}$ ) stress intensity factor at the middle surface of the shell was given as 2.42 by Erdogan [16]. The present method yielded a corresponding value of 2.4521, which is 1.3% higher than the exact solution. As a second example, a thick cylinder ( $R_o/t = 5$ ) with a part-through axisymmetric outer edge crack (crack depth/ $t = 0.5$ ) subjected to an axial stress of  $\sigma_o$  was analyzed. The solution of normalized (by  $\sigma_o\sqrt{\pi a}$ ) stress-intensity factor by the present approach was obtained as 1.7967, which is 6.8% higher than the exact solution of 1.6817 by Erdol and Erdogan [17]. The present procedure was also tested against the solution of an uncracked thin shell ( $R_o/t = 21$ ) with clamped edges and subjected to internal pressure and uniform temperature increase. The present solution for displacements as well as stresses agreed to within 5% of the exact solution given by Kraus [18], the present solution being higher than the exact solution. A detailed discussion of problem geometries, finite element breakdown and results of these problems along with detailed comparison with known exact solutions can be found in Atluri and Kathiresan [19].

**3.3 Belt-Line Surface Flaws in Pressure Vessels:** The presently considered meridional surface flaw problems, and the details of the corresponding finite element models are illustrated in Fig. 3. Results for normalized stress intensity factors for the two cases of  $a/(R_o - R_i) = .5$  and .8 are shown in Fig. 4 along with comparison results of [10,11]. It can be observed from the figure that the present solution agrees excellently with that of [10] for  $a/t = 0.8$  while there is a difference of 6% for  $a/t = 0.5$ , whereas, solution [11], by boundary integral equation method, agreed to within 10% and 0% of the present solution for  $a/t$  ratios of .5

and .8, respectively. A further study was made to investigate the effects of simulating the end condition of hemispherical end caps at the ends of the vessel in the finite element procedure; and the present solution dropped by about 3.5% along the crack front. The present solution is believed to be more accurate in the context of its excellent performance for surface flaw problems in thin plates and in problems with known exact solutions. Moreover, the use of Lamé's thick vessel solution for hoop stresses along the thickness direction of the vessel, by McGowan et al [10], may not be an accurate representation of the stresses, because the present vessel geometry is more close to being a thin shell.

With identical vessel geometry, the case of semi-elliptical surface flaws in the circumferential direction of the vessel are treated next. The finite element breakdown is similar to the one in Fig. 3, except that the meridional and circumferential lines are interchanged. The solutions for crack depth to cylinder thickness ratios of .5 and .8 and the case of internal pressure are presented in Fig. 5. The crack shapes are not exactly semi-elliptical in nature, but the real crack shapes used are illustrated in Fig. 5. From the solution of normalized stress intensity factors, it is clear that the case of circumferential surface flaws are not as severe as that of the meridional cracks for identical crack geometries. However, loads in the axial directions of the cylinder would be more critical in the case of circumferential crack. Thus the problem was also analyzed for uniform pressure on crack surface and the solutions of normalized stress intensity factors are also presented in Fig. 5.

3.4 Nozzle Corner Cracks in ITV and BWR Vessels: Two sample problems, an ITV and a BWR vessel with nozzle corner cracks, from the experimental investigation of Smith et al [1] were next considered for analysis by the present hybrid model. Natural flaw shapes as observed in experiments [1] were inserted in the finite element model. Thus the reader may obtain the geometries of the pressure vessel and cracks from the work of Smith et al [1]. A typical cross-sectional view of the finite element breakdown, which contains 452 total number of elements and 7677 total number (before imposition of boundary conditions) of degrees of freedom, is presented in Fig. 6. The solution of normalized stress intensity factors for the deepest natural flaw in ITV vessel (flaw shape No. 6 of Ref. [1]) is presented in Fig. 7. The figure contains the experimental solution [1] and the solutions by the present procedure for two Poisson's ratios, namely  $\nu = 0.3$  and  $0.45$ . Note that the photoelastic materials used in the experiments [1] are nearly incompressible ( $\nu \approx 0.5$ ). The solution corresponding to  $\nu = 0.45$  agrees well with the experimental solution [1] and had a 5% lower value at angle of rotation of  $45^\circ$ . Further, simulation of hemispherical end caps, in the finite element model, increased the value at mid-crack location by about 2.5%, thus improving the correlation with the experimental values. Smith et al [1,20] estimated that the experimental solutions may be higher than the solutions for materials with lower Poisson's ratio by a factor of  $\{(1-\nu)^2/(1-.5^2)\}^{1/2}$ . Thus for a material with  $\nu = 0.3$ , the experimental overestimation is about 10%, which is consistent with the solution corresponding to  $\nu = .3$  in Fig. 7.

As in the case of ITV models, several crack geometries in BWR vessels were also studied, using photoelasticity technique, by Smith et al [1]. An intermediate depth natural flaw shape ( $a/t = 0.57$  of Ref. [1]) was chosen to be analyzed by the present procedure. The finite element breakdown is similar to the one given in Fig. 6. The solutions of normalized

stress intensity factors by photoelasticity technique [1] and present method are presented in Fig. 8. The present solution appears to differ from that reported by Smith et al [1] except near the end points of the crack. The difference between these two sets of results at an angle of rotation of  $45^\circ$  is about 24%. The present solution corresponds to a Poisson's ratio of .45. Hemispherical end cap conditions were again simulated for these problems and there was no significant difference in the solution. The reasons for this discrepancy are currently being explored by refining the mesh of the finite element model, and by imposition of more accurate boundary conditions, etc. Several other crack geometries in BWR vessels as reported in [1] are also being investigated. These will be reported on in the very near future.

4. Conclusion: The hybrid displacement finite element model was applied to obtain the solutions of simple to complex three-dimensional fracture problems. The method demonstrated its potential by yielding excellent correlation with other available numerical as well as experimental solutions.

Acknowledgements: The results reported herein were obtained during the course of an investigation sponsored by HSST program under UCCND Subcontract 7565 between Union Carbide Corporation and Georgia Institute of Technology. The authors gratefully acknowledge this support.

References:

- [1] Smith, C. W., Peters, W. H. and Jolles, M. I., Journal of Pressure Vessel Technology, Transactions of the ASME, Vol. 100, No. 2, May 1978, pp. 141-150.
- [2] Hellen, T. K. and Dowling, A. R., International Journal of Pressure Vessels and Piping, Vol. 3, 1975, pp. 57-74.
- [3] Broekhoven, M. J. G., Third SMIRT, London, 1975, Paper No. G-4/6.
- [4] Broekhoven, M. J. G., Proceedings of the Third International Conference on Pressure Vessel Technology - Part II Materials and Fabrication, ASME, Tokyo, Japan, 1977, pp. 839-852.
- [5] Miyazono, S., Ueda, S., Kodaira, T., Shibata, K., Isozaki, T. and Nakajima, N., Proceedings of the Third International Conference on Pressure Vessel Technology - Part II Materials and Fabrication, ASME, Tokyo, Japan, 1977, pp. 741-748.
- [6] Schmitt, W., Bartholomé, G., Gröstad, A. and Miksch, M., International Journal of Fracture, Vol. 12, No. 3, June 1976, pp. 381-390.
- [7] Reynen, J., Third SMIRT, London, 1975, Paper No. G-5/1.
- [8] Atluri, S. N., Kathiresan, K. and Kobayashi, A. S., Third SMIRT, London, 1975, Paper No. L-7/3.
- [9] Atluri, S. N. and Kathiresan, K., Fourth SMIRT, San Francisco, 1977, Paper No. G-5/4.
- [10] McGowan, J. J. and Raymund, M., Proceedings of the Eleventh National Symposium on Fracture Mechanics, Blacksburg, Virginia, June 1978.
- [11] Heliot, J., Labbens, R. C. and Pellissier-Tanon, A., Proceedings of the Eleventh National Symposium on Fracture Mechanics, Blacksburg, Virginia, June 1978.
- [12] ASME Boiler and Pressure Vessel Code, Section III, Appendix G, 1977.
- [13] Raju, I. S. and Newman, J. C., Jr., Fourth SMIRT, San Francisco, 1977, Paper No. G-5/8.
- [14] Atluri, S. N. and Kathiresan, K., Nuclear Engineering and Design, Vol. 51, No. 2, January 1979, pp. 163-176.
- [15] Tracey, D. M., Nuclear Engineering and Design, Vol. 26, No. 2, 1974, pp. 282-290.
- [16] Erdogan, F., Mechanics of Fracture-Volume III Plates and Shells with Crack, Ed. by G. C. Sih, Noordhoff, The Netherlands, 1977.
- [17] Erdol, R. and Erdogan, F., Journal of Applied Mechanics, Transactions of the ASME, Vol. 45, June 1978, pp. 281-286.

- [18] Kraus, H., *Thin Elastic Shells*, John Wiley and Sons, New York, 1967.
- [19] Atluri, S. N. and Kathiresan, K., presented at the 3rd U.S. National Congress on Pressure Vessels and Piping, San Francisco, June 25-29, 1979.
- [20] Smith, C. W., McGowan, J. J. and Jolles, M. I., *Experimental Mechanics*, Vol. 16, No. 5, May 1976, pp. 188-193.

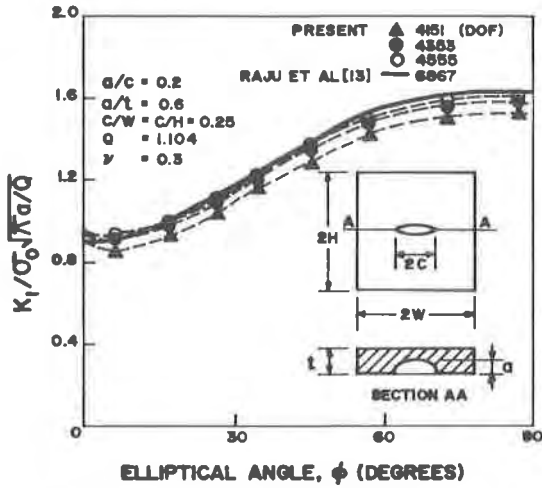


Fig.1. Solution for Surface Flaw in Thin Plates ( $a/t=0.6$ )

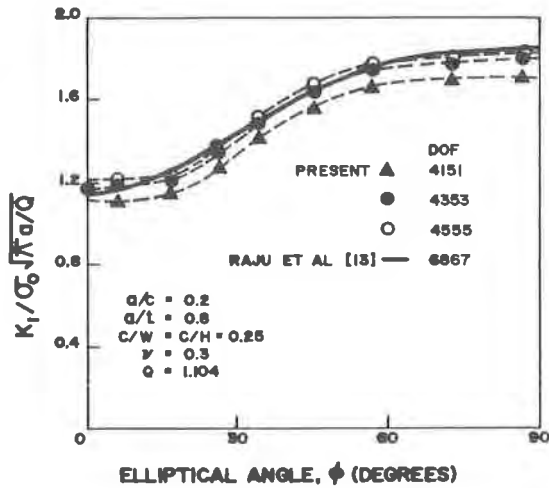


Fig.2. Solution for Surface Flaw in Thin Plates ( $a/t=0.8$ )

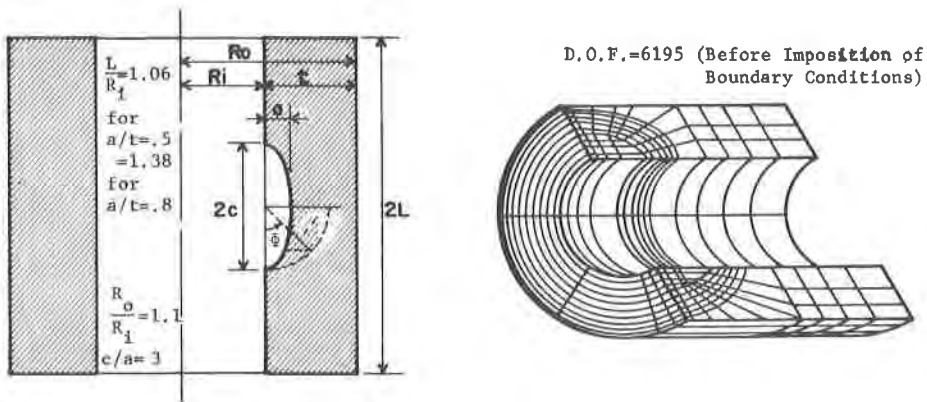


Fig. 3. Geometry and Finite Element Breakdown of Meridional Surface Flow Problems in Pressure Vessels

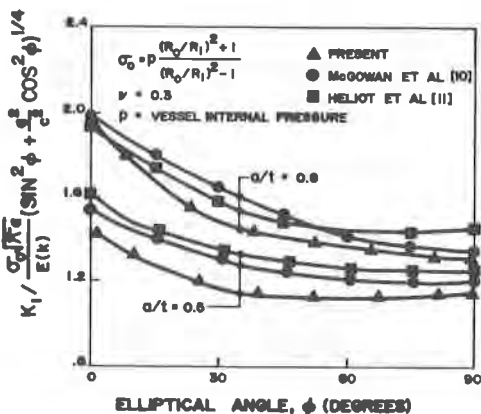


Fig. 4. Solution for Meridional Surface Flaws in Pressure Vessels

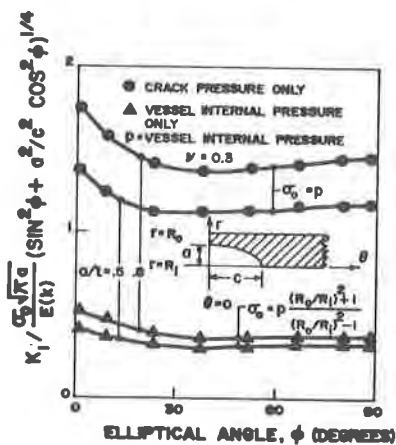


Fig. 5. Solution for Circumferential Surface Flaws in Pressure Vessels

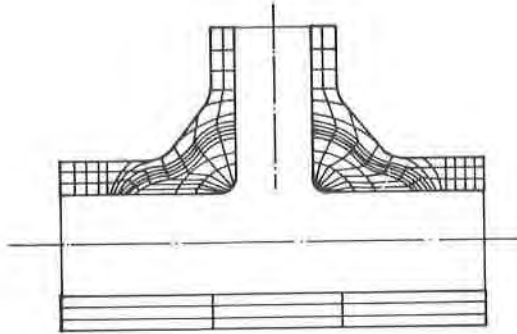


Fig. 6. Cross-sectional View of Finite Element Breakdown for Nozzle Corner Crack Problem

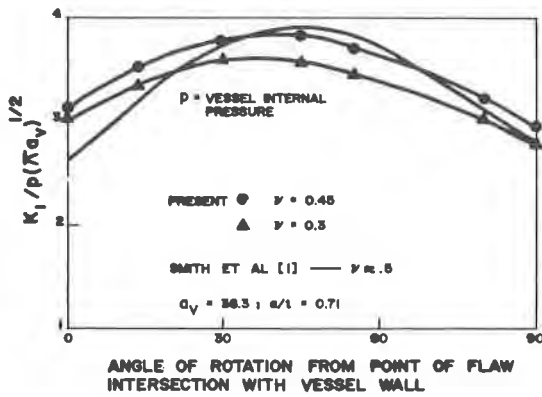


Fig. 7. Solution for Corner Crack at ITV Vessel-Nozzle Junction

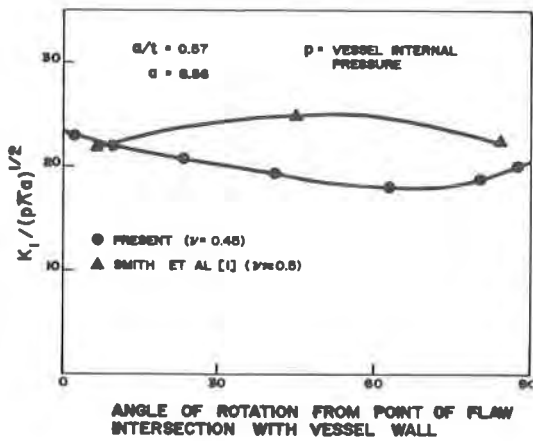


Fig. 8. Solution for Corner Crack at BWR Vessel-Nozzle Junction